Spin-liquid behavior in the spin-frustrated Mo_3 cluster magnet $Li_2ScMo_3O_8$ in contrast to magnetic ordering in isomorphic $Li_2InMo_3O_8$

Yuya Haraguchi,[1,*] Chishiro Michioka,[1,†] Masaki Imai,[1] Hiroaki Ueda,[1] and Kazuyoshi Yoshimura[1,2]
[1]*Department of Chemistry, Graduate School of Science, Kyoto University, Kyoto 606-8502, Japan*
[2]*Research Center for Low Temperature and Materials Sciences, Kyoto University, Kyoto 606-8501, Japan*
(Received 25 December 2014; revised manuscript received 5 June 2015; published 9 July 2015)

We synthesized the novel $S = 1/2Mo_3$ cluster magnet $Li_2ScMo_3O_8$ as well as the isomorphic compound $Li_2InMo_3O_8$, and investigated their macroscopic and microscopic physical properties. $Li_2InMo_3O_8$ showed magnetic ordering at $T_N \sim 12$ K with a 120° structure, while no magnetic ordering is observed down to 0.5 K in $Li_2ScMo_3O_8$ despite the strong antiferromagnetic interaction among clusters probed by the Weiss temperature. Results of the ^{7}Li nuclear magnetic resonance spectra and the nuclear spin-lattice relaxation rate ($1/T_1$) measurement show direct microscopic proof of the spin-disordered ground state. We discuss the difference in the ground state between $Li_2ScMo_3O_8$ and $Li_2InMo_3O_8$ using the description of localized magnetism based on spin frustration within the triangular lattice and that of inter- and intracluster charge fluctuations.

DOI: 10.1103/PhysRevB.92.014409 PACS number(s): 75.10.Jm, 75.40.−s, 76.60.−k

I. INTRODUCTION

Quantum spin frustrated magnets are expected to exhibit exotic ground states, for example, a resonating valence bond, a spin-liquid state, etc. [1–4]. In realistic compounds, the highly frustrated spin-liquid state is hard to realize owing to the higher order interactions and coupling to other degrees of freedom such as lattice, valence, and orbital instabilities. Newly produced ground states may contain novel physics depending on the characteristics of each compound.

So-called cluster magnets are defined as the spin system, in which several ions make magnetic moments with the overlap of their molecular orbitals. The physical properties of many cluster magnets have been investigated so far [5–9]. The design of a magnetic lattice with magnetic clusters in place of magnetic ions can produce novel magnetic spin systems. More specifically, the chemical discovery of cluster magnets with frustration lattices is expected to lead to a new frontier in the research field of novel spin frustration systems.

Recently, triangular lattice Mo_3 cluster antiferromagnetic systems have attracted intensive experimental and theoretical attention [10–14]. Various compounds, for example, $LiZn_2Mo_3O_8$ [15], $ScZnMo_3O_8$ [15], and $Li_2InMo_3O_8$ [16] have been discovered so far. As shown in Fig. 1(c), Mo_3 trimers form a quasi-two-dimensional triangular lattice in these compounds. Seven $4d$ electrons in the Mo_3 cluster occupy their orbitals, resulting in one unpaired spin per one Mo_3 cluster as shown in Fig. 1(a). As a concrete case of novel physics in the Mo_3 magnetic cluster systems, $LiZn_2Mo_3O_8$ exhibits the disappearance of 2/3 of the paramagnetic spins without the magnetic ordering, whose origin is believed to be the formation of a condensed valence-bond solid [10–12]. Flint and Lee suggested that $LiZn_2Mo_3O_8$ possibly has an emergent honeycomb lattice produced by the rotation of Mo_3O_{13} clusters and such a characteristic structure results in a plaquette valence bond solid state with orphan spins [13]. The plaquette valence bond solid state also appears in the phase diagram for the 1/6-filled extended Hubbard model [14]. As mentioned above, exotic properties are expected in Mo_3 cluster systems.

In this paper, we report on the synthesis of a new Mo_3 cluster compound $Li_2ScMo_3O_8$ and also an isomorphic compound $Li_2InMo_3O_8$ as well as the results of the magnetic susceptibility, heat capacity, and ^{7}Li nuclear magnetic resonance (NMR) investigations. $Li_2InMo_3O_8$ and $Li_2ScMo_3O_8$ have an isostructural magnetic cluster layer of $LiZn_2Mo_3O_8$ as shown in Fig. 1(c). The stacking structure of $Li_2InMo_3O_8$ and $Li_2ScMo_3O_8$ is shown in Fig. 1(b). The Mo_3 cluster layers of $Li_2InMo_3O_8$ and $Li_2ScMo_3O_8$ are sandwiched between countercations of Li^+ and A^{3+} (A = In or Sc). Although the compounds show similar physical properties at high temperatures, their ground states are completely different from each other; $Li_2InMo_3O_8$ exhibits a conventional magnetic ordering with a 120° structure, and $Li_2ScMo_3O_8$ exhibits a spin-liquid behavior.

II. EXPERIMENTAL METHODS

Polycrystalline samples of $Li_2InMo_3O_8$ and $Li_2ScMo_3O_8$ were prepared using conventional solid-state reactions from stoichiometric mixtures of Li_2MoO_4, In_2O_3/Sc_2O_3, MoO_3, and metallic Mo in an Ar atmosphere. As a starting material, metallic Mo was reduced by heating under a hydrogen stream before use.

These samples were characterized by powder x-ray diffraction (XRD) on a diffractometer (M18XHF, Mac Science) with Cu$K\alpha$ radiation. The cell parameters and the crystal structures were refined by the Rietveld method using RIETAN-FP v2.16 [17]. The temperature dependence of the magnetization was measured under several magnetic fields up to 7 T by using a magnetic property measurement system (MPMS; Quantum Design) equipped at the LTM Research Center, Kyoto University. The temperature dependence of the specific heat was measured by using a conventional relaxation method with a physical property measurement system (PPMS; Quantum Design). NMR measurements were carried out by observation of spin-echo and free induction decay (FID) signals with a standard phase-coherent-type

*chiyuya@kuchem.kyoto-u.ac.jp
†michioka@kuchem.kyoto-u.ac.jp

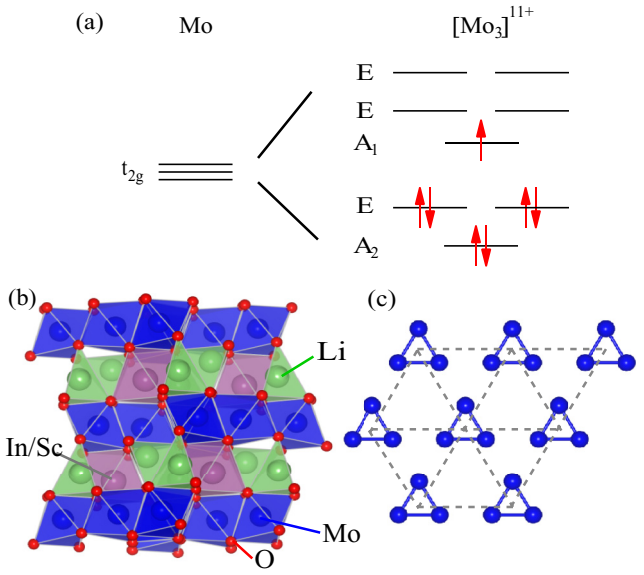

FIG. 1. (Color online) (a) Qualitative 4*d* orbital energy level schemes of the octahedrally coordinated Mo and the Mo_3 trimer with the electron configurations expected in $Li_2AMo_3O_8$. (b) Crystal structure of $Li_2AMo_3O_8$ viewed along the *b* axis. (c) $[Mo_3]^{11+}$ trimers forming the triangular lattice.

NMR-pulsed spectrometer. NMR spectra were measured by the fast Fourier transform method of spin echo and FID for the paramagnetic state and by plotting spin-echo intensities with sweeping frequency in a constant magnetic field for the magnetically ordered state. The nuclear spin-lattice relaxation rate $(1/T_1)$ was measured by the inversion recovery method. Here, the ^{7}Li nucleus with nuclear spin $I = 3/2$ has the nuclear gyromagnetic ratio $\gamma = 16.546$ MHz/T.

III. RESULTS AND DISCUSSION

The powder x-ray diffraction patterns of $Li_2InMo_3O_8$ and $Li_2ScMo_3O_8$ are shown in Fig. 2. All the indexed peaks without impurity peaks for both compounds can be characterized with the space group of $P6_3mc$. The structures of $Li_2InMo_3O_8$ and $Li_2ScMo_3O_8$ were refined by using the Rietveld method as described in the experimental section. Details of the refinement

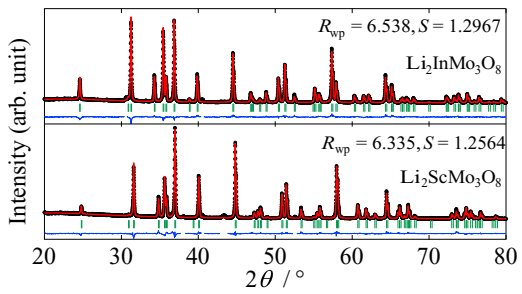

FIG. 2. (Color online) Powder x-ray diffraction patterns for $Li_2AMo_3O_8$. The filled circles are experimental data, and the vertical bars indicate the positions of Bragg reflections. The curve on the data shows a calculated pattern, and the bottom curve shows a deviation between the experimental and calculated intensities.

TABLE I. Crystallographic parameters for $Li_2InMo_3O_8$ and $Li_2ScMo_3O_8$ (both $P6_3mc$) determined using powder x-ray diffraction. The obtained lattice parameters are $a = 5.7846$ and 5.7732 Å and $c = 10.448$ and 10.288 Å, respectively, for $Li_2InMo_3O_8$ and $Li_2ScMo_3O_8$. *B* is the thermal displacement parameter.

	Site	*x*	*y*	*z*	*B* (Å)
$Li_2InMo_3O_8$					
Li1	2*a*	0	0	0.1678	0.6
Li2	2*b*	1/3	2/3	0.0825	0.6
In1	2*b*	1/3	2/3	0.6744	0.48
Mo1	6*c*	0.1876	0.8124	0.3931	0.34
O1	6*c*	0.5190	0.4810	0.0261	0.48
O2	6*c*	0.8421	0.1579	0.2940	0.41
O3	2*a*	0	0	0	0.40
O4	2*b*	1/3	2/3	0.2579	0.43
$Li_2ScMo_3O_8$					
Li1	2*a*	0	0	0.1689	0.6
Li2	2*b*	1/3	2/3	0.0836	0.6
Sc1	2*b*	1/3	2/3	0.6732	1.5
Mo1	6*c*	0.1870	0.8130	0.3916	0.17
O1	6*c*	0.5193	0.4807	0.0319	0.43
O2	6*c*	0.8429	0.1571	0.2862	0.40
O3	2*a*	0	0	0	0.45
O4	2*b*	1/3	2/3	0.2585	0.40

parameters are given in Table I. The large/small relation of the lattice parameters is consistent with the ionic radii of In^{3+} and Sc^{3+}. Mo atoms are strongly shifted from the center of the octahedral site to form Mo_3 trimers, which leads to two kinds of Mo-Mo distances: the short intracluster Mo-Mo distance d_{intra} and the long intercluster distance d_{inter}. The refined Mo-Mo distances are $d_{intra} = 2.529$ and 2.535 Å and $d_{inter} = 3.256$ and 3.239 Å, respectively, for $Li_2InMo_3O_8$ and $Li_2ScMo_3O_8$. The d_{intra} indicates the metallic bond within the intracluster to form the molecular orbital, and d_{inter} implies the absence of strong intercluster coupling. These compounds show an insulating behavior, indicating the localized character of unpaired electrons in the A_1 cluster orbital arranged in the center of the small Mo_3 trimer. Hence, the unpaired electrons have the $S = 1/2$ magnetic moment per Mo_3 cluster formed on a triangular lattice, as described in Fig. 1(c).

The temperature dependence of the magnetic susceptibility χ for $Li_2InMo_3O_8$ and $Li_2ScMo_3O_8$ are shown in Fig. 3. As shown in the inset, there is a linear relationship between $1/\chi$ and T at high temperatures. The Curie-Weiss fitting in the range from 200 to 300 K yields an effective paramagnetic Bohr magneton $p_{eff} = 1.61$ with the Weiss temperature $\Theta_W = -242$ K for $Li_2InMo_3O_8$, and $p_{eff} = 1.65$ with $\Theta_W = -127$ K for $Li_2ScMo_3O_8$. The deviation of p_{eff} for $Li_2AMo_3O_8$ from the ideal value of $p_{eff} = 1.73$ for $S = 1/2$ may be owing to the orbital contribution. The large and negative Θ_W indicates that the magnetic interactions are dominantly antiferromagnetic among spins of Mo_3 clusters. Note that the value of Θ_W in $Li_2InMo_3O_8$ is approximately two times larger than that in $Li_2ScMo_3O_8$. These antiferromagnetic couplings originate in the superexchange interaction between unpaired spins in the A_1 cluster orbitals of Mo_3 clusters. Possible exchange paths among Mo_3 clusters are Mo-O2-Mo and Mo-O3-Mo. In these

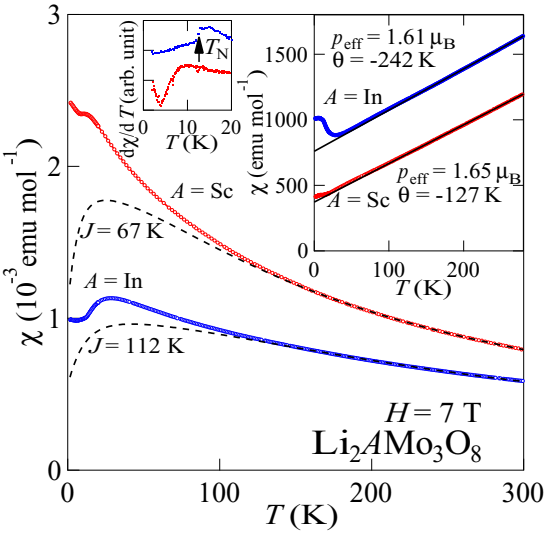

FIG. 3. (Color online) Temperature dependence of the magnetic susceptibility χ of $Li_2InMo_3O_8$ and $Li_2ScMo_3O_8$ under the applied magnetic field of 7 T. The broken lines show the result using 14th-order high-temperature expansions of the $S = 1/2$ Heisenberg triangular lattice model with the exchange interaction of $J = -112$ and -67 K, respectively, for $Li_2InMo_3O_8$ and $Li_2ScMo_3O_8$. The right inset shows the inverse magnetic susceptibility $1/\chi$. The left inset shows the low-temperature region of χ for $Li_2InMo_3O_8$ and $Li_2ScMo_3O_8$.

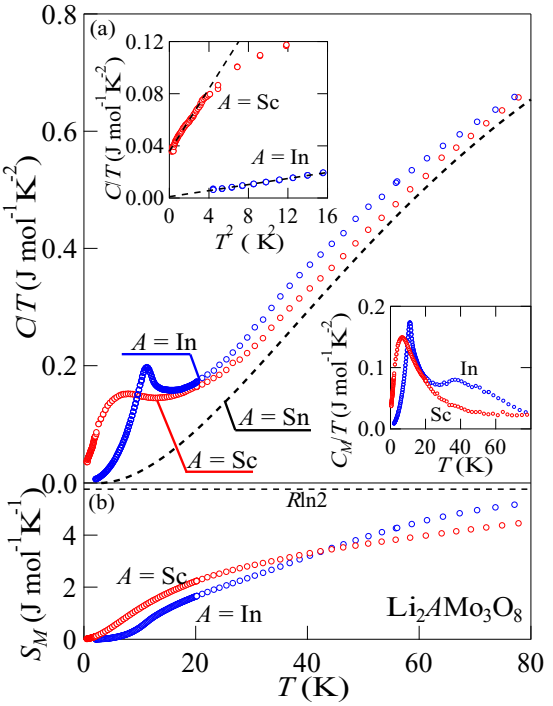

FIG. 4. (Color online) (a) Temperature dependence of the heat capacity divided by temperature C/T in $Li_2InMo_3O_8$, $Li_2ScMo_3O_8$, and the nonmagnetic isomorphic compound $Li_2SnMo_3O_8$. The top inset shows the C/T versus T^2 plot. The bottom inset displays C_M/T of $Li_2InMo_3O_8$ and $Li_2ScMo_3O_8$ obtained by subtracting the lattice contribution estimated from C/T of $Li_2SnMo_3O_8$. (b) Temperature dependence of the magnetic entropy S_M. The horizontal dashed line indicates $S_M = R \ln 2$.

compounds, these bond angles are ∠Mo-O2-Mo = 96.24° and 96.11°, ∠Mo-O3-Mo = 106.36° and 104.33°, respectively, for $Li_2InMo_3O_8$ and $Li_2ScMo_3O_8$. The slight deviation in these bond angles between $Li_2InMo_3O_8$ and $Li_2ScMo_3O_8$ cannot explain the large difference between the Θ_W values of $Li_2InMo_3O_8$ and $Li_2ScMo_3O_8$ by the simple Kanamori theory [18]. This fact indicates that higher-order exchange interactions are effective.

In the low-temperature region, χs for $Li_2InMo_3O_8$ and $Li_2ScMo_3O_8$ do not obey the Curie-Weiss law and have local maxima around 29 and 10 K, respectively, suggesting the development of short-range ordering owing to the low dimensionality and/or the spin frustration effect. The broken lines in Fig. 3 are the result of fitting by using the theoretical equation of the two-dimensional (2D) $S = 1/2$ Heisenberg triangular lattice antiferromagnet in the range from 200 to 300 K [19]. In the low-temperature region, the 2D $S = 1/2$ Heisenberg triangular lattice antiferromagnet model deviates from the observed χ. There are three possible explanations for the deviation of χ: the existence of the higher-order exchange interactions, the three dimensionality from the existence of weak couplings between cluster layers, and the magnetic anisotropy owing to partial unquenched orbital contributions.

As shown in the left inset of Fig. 3, the temperature derivative χ for $Li_2InMo_3O_8$ bends steeply and $d\chi/dT$ decreases discontinuously at ∼12 K indicating the presence of long-range ordering, which is confirmed by the result of heat capacity and ^{7}Li-NMR measurements as mentioned below. In contrast, $d\chi/dT$ for $Li_2ScMo_3O_8$ does not show any discontinuous changes down to 2 K. To clarify the properties of different ground states between $Li_2InMo_3O_8$ and $Li_2ScMo_3O_8$, we measured the specific heat C.

Figure 4(a) shows the temperature dependence of the specific heat divided by temperature (C/T) for $Li_2InMo_3O_8$ and $Li_2ScMo_3O_8$. In the case of $Li_2InMo_3O_8$, the λ-shaped peak was observed at the same temperature where $d\chi/dT$ shows the discontinuous drop, suggesting the existence of long-range ordering. In the case of $Li_2ScMo_3O_8$, we observed no λ-typed anomaly in C/T down to 0.5 K but only a broad hump near 10 K, indicating the absence of any magnetic orderings, which is consistent with the temperature dependence of χ. The C/T versus T^2 plot of $Li_2ScMo_3O_8$ at temperatures below 4 K is shown in the inset of Fig. 4. The existence of a linearly temperature dependent γ term is clearly verified. The magnitude of γ is estimated as 35.7 mJmol^{-1}K^{-2}. On the other hand, the linear extrapolation to $T = 0$ for C/T of $Li_2InMo_3O_8$ with the magnetic ordering ground state gives a vanishing γ term. The χ of $Li_2ScMo_3O_8$ does not show a difference between the zero-field-cooling and field-cooling process. These facts suggest that the magnetic entropy remains at a low temperature owing to the spin frustration effect in $Li_2ScMo_3O_8$.

The bottom inset of Fig. 4(a) shows the magnetic heat capacity divided by temperature, C_M/T, of $Li_2InMo_3O_8$ and $Li_2ScMo_3O_8$ after subtraction of their lattice contributions estimated from C/T of the nonmagnetic isomorphic

compound $Li_2SnMo_3O_8$. C_M/T of $Li_2InMo_3O_8$ exhibits two peaks: a sharp peak at $T_N \sim 12$ K and an extra broad peak at $T \sim 39$ K indicating the existence of short-range orderings, which is consistent with the broad maximum behavior of χ in $Li_2InMo_3O_8$. On the other hand, in the case of $Li_2ScMo_3O_8$, C_M/T shows only a single broad hump at $T \sim 10$ K with a small shoulder at ~ 20 K due to the development of antiferromagnetic short-range orderings. Figure 4(b) shows the magnetic entropy S_M calculated by integrating C_M/T. In the case of $Li_2InMo_3O_8$, S_M reaches approximately 0.67 $Jmol^{-1}\,K^{-1}$ at T_N. This value is 12% of the ideal total magnetic entropy $R\ln 2$ derived from $S = 1/2$. Thus, a large part of magnetic entropy is released with the short-range magnetic correlation above T_N owing to the spin frustration effect. On the other hand, S_M of $Li_2ScMo_3O_8$ gradually increases with increasing temperature. In the case of $LiZn_2Mo_3O_8$, S_M has a plateau at approximately $1/3R\ln 2$ indicating the disappearance of 2/3 of the paramagnetic spins without magnetic orderings [10]. Sheckelton *et al.* proposed that the disappearance is attributed to the construction of a valence-bond solid on the honeycomb sublattice. In the case of $Li_2ScMo_3O_8$, such a plateau was not observed, suggesting that the spin-disordered ground state of $Li_2ScMo_3O_8$ is different from that of $LiZn_2Mo_3O_8$. The magnetic entropies at 80 K reach 5.2 and 4.5 $J\,mol^{-1}\,K^{-1}$, respectively, for $Li_2InMo_3O_8$ and $Li_2ScMo_3O_8$. Their values correspond to 90% and 78% of the expected total entropy, respectively.

Figure 5 shows the ^{7}Li-NMR spectra for $Li_2AMo_3O_8$ (A = In, Sc) measured at 300 K and approximately 1.22 T. The data presented in light blue are the raw data. The black, blue, and red lines denote the simulated spectra for Li(1), Li(2), and the sum of them, respectively. The parameters of ν_Q, η, K_{iso}, and K_{aniso} are also shown in the figure. Good agreement between experimental and simulated spectra suggests that there is little randomness to the Li sites in these compounds.

The ^{7}Li-NMR spectra for both compounds do not change significantly above 20 K. The spectra are broadened according to the Curie-Weiss-like enhancement of the magnetic susceptibility. The center peaks of both compounds shift very slightly to a lower frequency with decreasing temperature. This is not proportional to the magnetic susceptibility. Therefore, for the Li sites, the transferred hyperfine field is very small and the hyperfine field dominantly consists of the dipole field from the spins of Mo_3O_{13} clusters. In the case of the dipole field, the sum of the hyperfine coupling constants of A_{XX}, A_{YY}, A_{ZZ} is zero, resulting in the idea that the center of gravity in the spectrum is independent of the magnetic susceptibility. For both Li(1) and Li(2) sites, A_{ZZ} is larger than A_{XX} and A_{YY}. This fact and/or the temperature dependence of the chemical shift may be responsible for the slight temperature dependence of the center line.

Figure 6(a) shows the ^{7}Li-NMR spectra of $Li_2InMo_3O_8$ measured at 4.2 and 300 K and that of $Li_2ScMo_3O_8$ at 4.2 K for comparison. At 4.2 K, in contrast to the case of $Li_2ScMo_3O_8$, in which the spectrum is broadened only by the enhancement of the magnetic susceptibility, the spectrum shows strong broadening in the case of $Li_2InMo_3O_8$, suggesting the presence of an internal field due to the magnetic ordering. Figure 6(b) shows a comparison between the raw and simulated spectra, with an assumption of the 120° magnetic structure. We also

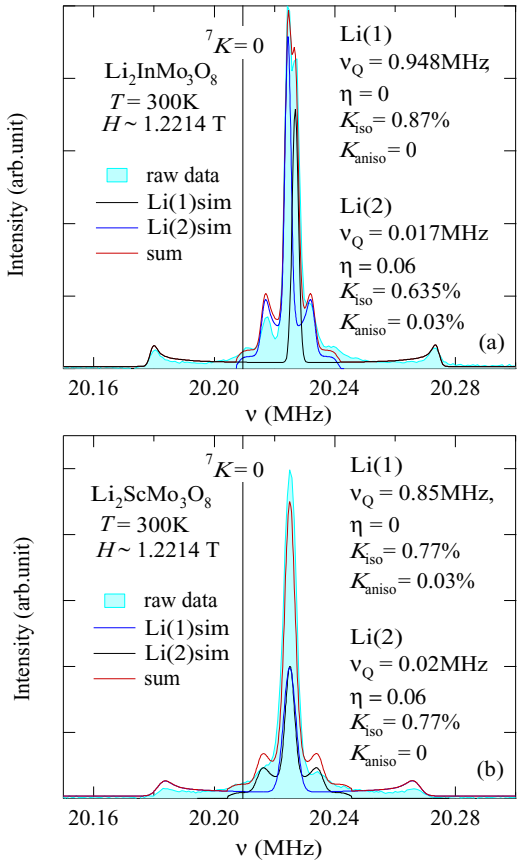

FIG. 5. (Color online) ^{7}Li-NMR spectra of (a) $Li_2InMo_3O_8$ and (b) $Li_2ScMo_3O_8$ measured at 300 K and in the external field of approximately 1.22 T. The data highlighted in light blue, and the black, blue, and red lines denote the raw data, the simulated spectra for Li(1), Li(2), and the sum of them, respectively.

assumed that the ordered magnetic moment of $0.895\mu_B$ which is close to the value of $S = 1/2$ spin is present in the center of the cluster and the hyperfine field is due only to the dipole-dipole interaction. Not limited in the case of the 120° structure, the powder pattern of the NMR spectrum would show a rectangular shape in the case of the commensurate magnetic structure. As shown in Fig. 6(b) the simulated spectrum for Li(1) can be reproduced by the rectangular-shaped spectrum due to the internal field with broadening factors by the magnetic susceptibility and the quadrupole interaction. For the Li(2) site, the internal field is almost canceled by itself, and the spectrum does not spread very much. Since the simulated spectrum does not depend on the magnetic stacking structure, the magnetic relationship in the ordered state between Mo layers in the unit cell cannot be determined uniquely from the ^{7}Li-NMR data by using a polycrystalline sample. From these facts, we can summarize the information about the magnetic structure as follows: (1) In a Mo cluster layer, spins form the 120°structure. (2) The magnetic unit cell along the stacking direction is possibly the same as the crystallographic unit cell. (3) The interlayer magnetic structure in a unit cell is still unknown.

Figures 7(a) and 7(b) show the temperature dependence of the nuclear spin-lattice relaxation rate $(1/T_1)$ of $Li_2AMo_3O_8$

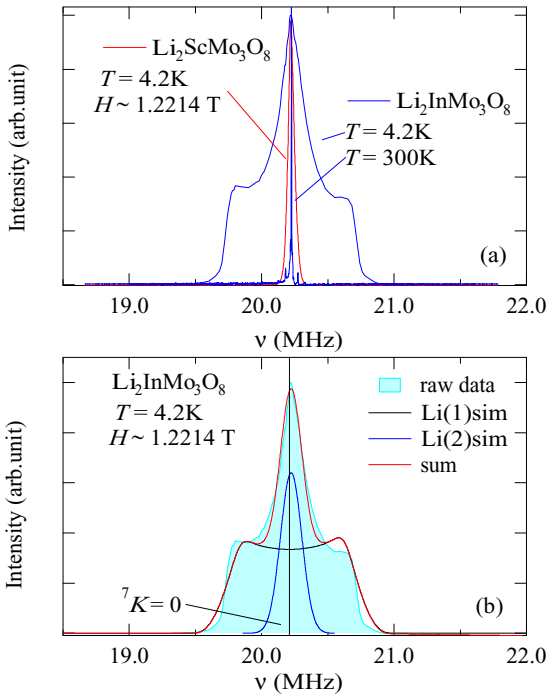

FIG. 6. (Color online) ^{7}Li-NMR spectra of (a) $Li_2InMo_3O_8$ at 4.2 and 300 K and that of $Li_2ScMo_3O_8$ at 4.2 K. (b) Raw and simulated spectra for $Li_2InMo_3O_8$ at 4.2 K. The spectra highlighted in light blue, and the black, blue, and red lines denote the raw data, the simulated data for Li(1), Li(2), and the sum of them, respectively, with the assumption of the 120° structure (see text).

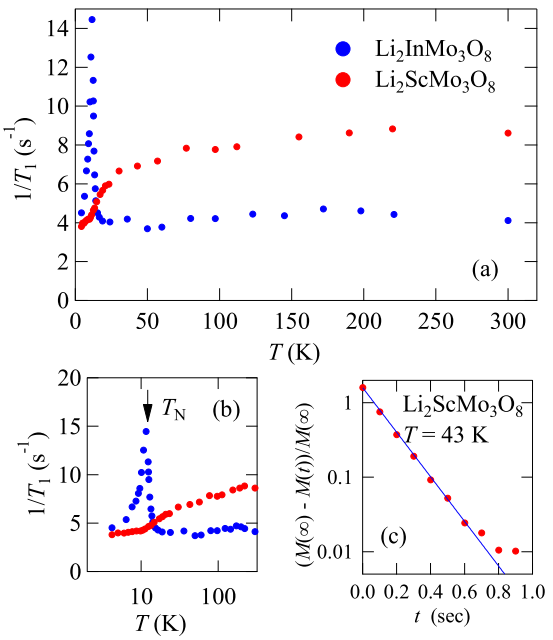

FIG. 7. (Color online) Temperature dependence of the nuclear spin-lattice relaxation rate ($1/T_1$) of $Li_2AMo_3O_8$ (A = In,Sc) with (a) linear and (b) semilogarithmic scales. (c) The recovery curve of $Li_2ScMo_3O_8$ measured at 43 K.

(A = In,Sc) with the linear and semilogarithmic scales, respectively. A typical example of the recovery curve is shown in Fig. 7(c). In both compounds with A = In or Sc, except for the magnetically ordered state, recovery curves almost follow the single exponential function $[M(\infty) - M(t)]/M(\infty) \propto \exp(-t/T_1)$, where t is the time duration between the inversion and observation pulses. This fact suggests two points. One is that the relaxation time (T_1) is approximately the same at both the Li(1) and Li(2) sites. Second, as an initial condition, all signals including the center and the satellite signals can be reversed by the inversion pulse. Owing to these facts, fortunately, T_1 can be determined almost uniquely.

In the case of $Li_2InMo_3O_8$, $1/T_1$ is nearly independent of temperature above 50 K. Such a behavior is typical in the case of the localized moment system far above the critical temperature indicating Curie's law, in which $1/T_1T$ is proportional to the uniform susceptibility. With decreasing temperature, $1/T_1$ is markedly enhanced and shows divergent behavior at $T_N \sim 12$ K. This is also strong evidence for the magnetic ordering. From ^{7}Li-NMR investigations, all these facts are found to be due to magnetic ordering with the 120° structure. Broad maximum behavior around 25 K in the χ versus T curve, which is expected to be a sign of magnetic ordering in the previous report [16], is possibly owing to a magnetic short-range ordering (correlation) due to the spin frustration.

In the case of $Li_2ScMo_3O_8$, while χ shows a similar behavior with that of $Li_2InMo_3O_8$, any signs of magnetic orderings are not observed in the temperature dependence of $1/T_1$. This result is consistent with the NMR spectrum measurement shown in Fig. 6(a). In addition, the heat capacity does not show any λ-type anomalies in its temperature dependence down to 0.5 K but shows a broad humplike anomaly around 10 K. The temperature dependence of $1/T_1$ rapidly drops below about 20 K, where χ deviates from the Curie-Weiss law, and shows an anomaly at about 10 K. These behaviors, at least that around 10 K, are possibly owing to the development of short-range spin correlations.

Here we discuss the origin of the difference of the magnetism for $Li_2AMo_3O_8$ and $LiZn_2Mo_8O_8$. There are two major differences. One is the deviation of the p_{eff} value at high temperatures, and the other is the low-temperature behavior of χ.

As previously mentioned, the values of $p_{eff} = 1.61$ and 1.65, respectively, for $Li_2InMo_3O_8$ and $Li_2ScMo_3O_8$, are close to the expected spin-only contributed value of 1.73 for $S = 1/2$, while $p_{eff} = 1.39$ of $LiZn_2Mo_3O_8$ is quite small compared with the ideal value. One possible reason for the reduction of p_{eff} is the difference in partially unquenched orbital contributions. In addition, the crystallographical site defect possibly reduces the formal valence of $[Mo_3]^{11+}$. Indeed, in the case of $LiZn_2Mo_3O_8$, previous investigations clarified the existence of the crystallographical disorder of Li and Zn ions [11,15]. On the other hand, in $Li_2AMo_3O_8$, there is little randomness in the Li sites probed by XRD and the ^{7}Li-NMR spectrum.

The different low-temperature behaviors of χ for $Li_2AMo_3O_8$ and $LiZn_2Mo_8O_8$ would reflect developments of different short-range orderings. In $Li_2AMo_3O_8$, the broad maximum of the temperature derivative χ indicates the

development of short-range orderings with the 120° structure and/or those of two dimensionality. In $LiZn_2Mo_8O_8$, the temperature dependence of χ displays an apparent loss of the Curie constant without any maximum behavior interpreted by the construction of a valence bond solid [10]. Possible factors determining their ground states are different orbital contributions, lattice fluctuations including crystallographical disorder, and the balance of the charge fluctuations.

Finally, we discuss the ground state of $Li_2ScMo_3O_8$ without any magnetic orderings while using the quantum spin-liquid (QSL) description. The magnetic behaviors of $Li_2InMo_3O_8$ and $Li_2ScMo_3O_8$ at high temperatures are similar, which reflects that their magnetism is based on a similar spin model. However, their ground states are completely different from each other; while $Li_2InMo_3O_8$ exhibits a conventional magnetic ordering with a 120° structure, $Li_2ScMo_3O_8$ does not show any signs of magnetic orderings. In $Li_2ScMo_3O_8$, the residual γ term in the heat capacity and the sharp drop in $1/T_1$ possibly indicate the spin condensation of the QSL. The finite γ term could be explained by the gapless excitation around the spinon Fermi surface [20], where value is comparable to those of other QSL candidates with the triangular lattice such as κ-(BEDT-TTF)$_2$Cu$_2$(CN)$_3$ [21], EtMe$_3$Sb[Pd(dmit)$_2$]$_2$ [22], and $Ba_3CuSb_2O_9$ [23]. $Li_2ScMo_3O_8$ is a strong candidate of the QSL compound based on a triangular lattice antiferromagnet, which is in contrast to the isomorphic $Li_2InMo_3O_8$ with the magnetic ordering.

In the theory proposed by Chen *et al.* and using the single-band extended Hubbard model with electron hopping and Coulomb interactions within intra- and interclusters, the existence of two types of possible ground states is predicted: the plaquette charge order (PCO) and the QSL [14]. In this theory, the PCO state may explain the disappearance of 2/3 of the paramagnetic spins in $LiZn_2Mo_3O_8$. On the other hand, this theory predicted that the ground state is expected to be the U(1) QSL when the intra- and intercluster hopping and Coulomb interactions become more anisotropic. This model is powerful in treating inter- and intracluster charge fluctuations. However, this model cannot describe the strict localized spin magnetism in the strong Mott regime because of the lack of the treatment of the higher-order magnetic exchange interactions among cluster spins. $Li_2InMo_3O_8$ is located in the strong Mott regime in this model. Hence, its ground state is a magnetically ordered state with 120° structure. In the case of $Li_2ScMo_3O_8$, if this compound is in the strong Mott regime, the disordered ground state would be caused by the spin frustration effect, which has attracted much attention over the past several decades. If this compound is located in the weak Mott regime, such charge fluctuations possibly stabilize the U(1) QSL as the ground state as predicted with this theory [14]. Another possible scenario to stabilize the quantum spin-liquid state in $Li_2ScMo_3O_8$ is the emergence of honeycomb sublattice induced by lattice fluctuations, which are predicted by Flint and Lee [13]. Which model is dominant cannot be determined at present. It is necessary to perform precise microscopic structural studies such as inelastic x-ray scattering experiments in order to determine the existence/absence of such fluctuations. This is a matter for future research.

IV. SUMMARY

We have presented the structural parameters and macroscopic and microscopic physical properties of triangular lattice antiferromagnetic cluster compounds $Li_2InMo_3O_8$ and newly discovered $Li_2ScMo_3O_8$. It was found that while $Li_2InMo_3O_8$ is magnetically ordered at $T_N \sim 12$ K with the 120° structure, $Li_2ScMo_3O_8$ does not show any magnetic ordering within the measured temperature range. In $Li_2ScMo_3O_8$, the existence of a finite γ term in the heat capacity and the rapid drop in the nuclear spin-lattice relaxation rate strongly suggests that this compound is a QSL candidate realized on the spin-frustrated triangular lattice Heisenberg antiferromagnet, which is in contrast to magnetic ordering based on a similar spin model in $Li_2InMo_3O_8$.

ACKNOWLEDGMENTS

We thank N. Todoroki at Chiba Institute of Technology for the helpful discussions. This work was supported by Grants-in-Aid for Scientific Research from the Japan Society for Promotion of Science (Grant No. 26410089).

[1] P. W. Anderson, Mater. Res. Bull. **8**, 153 (1973).
[2] R. Moessner and S. L. Sondhi, Prog. Theor. Phys. Suppl. **145**, 37 (2002).
[3] P. A. Lee, Science **321**, 1306 (2008).
[4] L. Balents, Nature (London) **464**, 199 (2010).
[5] M. M. Abd-Elmeguid, B. Ni, D. I. Khomskii, R. Pocha, D. Johrendt, X. Wang, and K. Syassen, Phys. Rev. Lett. **93**, 126403 (2004).
[6] R. Pocha and D. Johrendt, Chem. Mater. **12**, 2882 (2000).
[7] H. Nakamura, H. Chudo, and M. Shiga, J. Phys.: Condens. Matter **17**, 6015 (2005).
[8] Y. Haraguchi, C. Michioka, H. Ueda, and K. Yoshimura, Phys. Rev. B **90**, 064403 (2014).
[9] E. V. Anokhina, C. S. Day, and A. Lachgar, Inorg. Chem. **40**, 5072 (2001).
[10] J. P. Sheckelton, J. R. Neilson, D. G. Soltan, and T. M. McQueen, Nat. Mater. **11**, 493 (2012).
[11] J. P. Sheckelton, F. R. Foronda, L. D. Pan, C. Moir, R. D. McDonald, T. Lancaster, P. J. Baker, N. P. Armitage, T. Imai, S. J. Blundell, and T. M. McQueen, Phys. Rev. B **89**, 064407 (2014).
[12] M. Mourigal, W. T. Fuhrman, J. P. Sheckelton, A. Wartelle, J. A. Rodriguez-Rivera, D. L. Abernathy, T. M. McQueen, and C. L. Broholm, Phys. Rev. Lett. **112**, 027202 (2014).
[13] R. Flint and P. A. Lee, Phys. Rev. Lett. **111**, 217201 (2013).
[14] G. Chen, H.-Y. Kee, and Y. B. Kim, arXiv:1504.01396.

[15] C. C. Torardi and R. E. McCarley, Inorg. Chem. **24**, 476 (1985).
[16] P. Gall, R. A. R. A. Orabi, T. Guizouarn, and P. Gougeon, J. Solid State Chem. **208**, 99 (2013).
[17] F. Izumi and K. Momma, Solid State Phenom. **130**, 15 (2007).
[18] J. Kanamori, J. Phys. Chem. Solids **10**, 87 (1959).
[19] M. Tamura and R. Kato, J. Phys.: Condens. Matter **14**, L729 (2002).
[20] C. P. Nave and P. A. Lee, Phys. Rev. B **76**, 235124 (2007).
[21] S. Yamashita, Y. Nakazawa, M. Oguni, Y. Oshima, H. Nojiri, Y. Shimizu, K. Miyagawa, and K. Kanoda, Nat. Phys. **4**, 459 (2008).
[22] S. Yamashita, T. Yamamoto, Y. Nakazawa, M. Tamura, and R. Kato, Nat. Commun. **2**, 275 (2011).
[23] H. D. Zhou, E. S. Choi, G. Li, L. Balicas, C. R. Wiebe, Y. Qiu, J. R. D. Copley, and J. S. Gardner, Phys. Rev. Lett. **106**, 147204 (2011).